PTEP

Prog. Theor. Exp. Phys. **2019**, 123B01 (21 pages)
DOI: 10.1093/ptep/ptz123

Exponentially suppressed cosmological constant with enhanced gauge symmetry in heterotic interpolating models

H. Itoyama[1,2,3,*] and Sota Nakajima[2,*]

[1] *Nambu Yoichiro Institute of Theoretical and Experimental Physics (NITEP), Osaka City University, 3-3-138, Sugimoto, Sumiyoshi-ku, Osaka 558-8585, Japan*
[2] *Department of Mathematics and Physics, Graduate School of Science, Osaka City University, 3-3-138, Sugimoto, Sumiyoshi-ku, Osaka 558-8585, Japan*
[3] *Osaka City University Advanced Mathematical Institute (OCAMI), 3-3-138, Sugimoto, Sumiyoshi-ku, Osaka 558-8585, Japan*
[*] E-mail: itoyama@sci.osaka-cu.ac.jp, sotanaka@sci.osaka-cu.ac.jp

Received June 13, 2019; Revised September 24, 2019; Accepted October 9, 2019; Published December 3, 2019

A few 9D interpolating models with two parameters are constructed and the massless spectra are studied by considering compactification of heterotic strings on a twisted circle with a Wilson line. It is found that there are some conditions between radius R and Wilson line A under which the gauge symmetry is enhanced. In particular, when the gauge symmetry is enhanced to $SO(18) \times SO(14)$, the cosmological constant is exponentially suppressed. We also construct a non-supersymmetric string model that is tachyon-free in all regions of moduli space and whose gauge symmetry involves E_8.

Subject Index B41

1. Introduction

LHC experiments suggest that supersymmetry (SUSY) does not exist at low-energy scales. It is, therefore, natural to consider the possibility that SUSY is broken at the string/Planck scale. For this reason, non-supersymmetric string models [1–3], in particular, the $SO(16) \times SO(16)$ heterotic string model, which is the unique tachyon-free 10D non-supersymmetric model, have been receiving more and more attention. Non-supersymmetric string models, however, always have a problem of stability. Unlike supersymmetric ones, the cosmological constant is non-vanishing. There are non-vanishing dilaton tadpoles that lead to vacuum instability. Thus, the desired model must be both non-supersymmetric and carry a very small cosmological constant. While several methods to construct such models have been proposed [4–11], in this paper, we try to construct non-supersymmetric heterotic models with a small cosmological constant by focusing on so-called interpolating models [12–15].

An interpolating model is a $(D-d)$-dimensional model that continuously relates two D-dimensional models. In this work, we restrict our attention to the case with $D = 10$ and $d = 1$ for simplicity. The method of constructing such models is as follows: We start from a 10D closed string model (called model M_1) and compactify this on a circle with a $\boldsymbol{Z}_2$ twist, which is nothing but the Scherk–Schwarz compactification [16,17]. The resulting 9D model should have a circle radius R as a parameter, which can be adjusted freely. Because we are considering closed string models, this 9D model

Funded by SCOAP^3

should produce a 10D model (called model M_2) in the $R \to 0$ limit as well due to T-duality [18,19]. In particular, if model M_1 is supersymmetric and the $\boldsymbol{Z}_2$ action contains $(-1)^F$ where F is the spacetime fermion number, the compactification causes SUSY breaking and the 9D interpolating model and model M_2 become non-supersymmetric.

In Refs. [12,20–22], it is shown that in the near-supersymmetric region of moduli space, the cosmological constant Λ_{10} is written as follows:

$$\Lambda_{10} \simeq (N_F - N_B)\xi \tilde{a}^8 + \mathcal{O}(e^{-\tilde{a}^2}), \tag{1}$$

where ξ is a positive constant and $\tilde{a} = a^{-1} = R/\sqrt{\alpha'}$, and N_F (N_B) is the number of massless fermionic (bosonic) degrees of freedom. Therefore, the cosmological constant is exponentially suppressed when $N_F = N_B$. We would like to have non-supersymmetric models with $N_F = N_B$, but the 9D interpolating models with one parameter R, which we will review in Sect. 2, do not have such a property no matter how one adjusts the parameter R. In order to generate cases with $N_F - N_B = 0$, we need to increase the number of adjustable parameters. One such possibility is to compactify more dimensions. In this work, we instead consider 9D interpolating models with one more parameter by introducing a constant Wilson line background.

2. Interpolating models with no Wilson line

In this section, we review the construction of an interpolating model that was originally proposed in Ref. [12], and provide two concrete examples. In these examples, we provide the interpolations between the 10D non-supersymmetric $SO(16) \times SO(16)$ heterotic string model and one of the 10D supersymmetric heterotic strings [23] as model M_2. The presentation below is based on Refs. [13,14].[1]

2.1. *The construction of interpolating models*

Let us start from a flat 10D closed string model M_1 whose partition function is

$$Z_{M_1} = Z_B^{(8)} Z_+^+, \tag{2}$$

where Z_+^+ represents the contribution from the fermionic and the internal parts of the string and $Z_B^{(n)}$ that from the bosonic parts of the string:

$$Z_B^{(n)} = \tau_2^{-n/2} (\eta\bar{\eta})^{-n}. \tag{3}$$

Let us first consider the circle compactification:

$$X^9 \sim X^9 + 2\pi R. \tag{4}$$

The left- and right-moving momenta along the compactified dimension are respectively

$$p_L = \frac{1}{\sqrt{2\alpha'}}\left(na + \frac{w}{a}\right), \quad p_R = \frac{1}{\sqrt{2\alpha'}}\left(na - \frac{w}{a}\right), \tag{5}$$

for $n, w \in \boldsymbol{Z}$. After the circle compactification, the partition function of model M_1 becomes

$$Z_+^{(9)+} = \left((\eta\bar{\eta})^{-1} \sum_{n,w\in\boldsymbol{Z}} q^{\frac{\alpha'}{2}p_L^2} \bar{q}^{\frac{\alpha'}{2}p_R^2}\right) Z_B^{(7)} Z_+^+. \tag{6}$$

[1] We can also construct these 9D string models by using free-fermionic construction [24–26].

In order to obtain two different 10D models at $R \to \infty$ and $R \to 0$ limits, we have to consider the compactification on a twisted circle. We choose $\mathcal{T}Q$ as the $\boldsymbol{Z}_2$ twist where $\mathcal{T}$ acts on the compactified circle as a half translation:

$$\mathcal{T} : \tilde{X}^9 \to \tilde{X}^9 + \pi \tilde{R}. \tag{7}$$

Here, $\tilde{X}^9$ is the T-dualized coordinate for the compactified dimension and $\tilde{R} = \alpha'/R$ is the T-dualized radius.[2] We denote by Q a $\boldsymbol{Z}_2$ action that acts on the internal part of the string and that determines the two 10D models at the limits.

Because the $\boldsymbol{Z}_2$ twist contains $\mathcal{T}$, the partition function of the interpolating model contains a set of four momentum lattices:

$$\begin{aligned}\Lambda_{\alpha,\beta} &\equiv (\eta\bar{\eta})^{-1} \sum_{n\in \boldsymbol{Z}+\alpha,\ w\in 2(\boldsymbol{Z}+\beta)} q^{\frac{\alpha'}{2}p_L^2} \bar{q}^{\frac{\alpha'}{2}p_R^2} \\ &= (\eta\bar{\eta})^{-1} \sum_{n,w\in \boldsymbol{Z}} \exp\left[-\pi \left\{\tau_2 \left(a^2(n+\alpha)^2 + 4a^{-2}(w+\beta)^2\right) - 4i\tau_1 (n+\alpha)(w+\beta)\right\}\right],\end{aligned} \tag{8}$$

where α and β are 0 or 1/2, and $\alpha = 0\,(1/2)$ and $\beta = 0\,(1/2)$ imply the integer (half-integer) momenta and the even (odd) winding numbers respectively. It is easy to show that under $\boldsymbol{T} :\ \tau \to \tau + 1$, $\Lambda_{\alpha,\beta}$ transforms as

$$\boldsymbol{T} :\ \Lambda_{\alpha,\beta} \to e^{4\pi i \alpha\beta} \Lambda_{\alpha,\beta}. \tag{9}$$

Under $\boldsymbol{S} : \tau \to -1/\tau$, by using the Poisson resummation formula, we obtain

$$\boldsymbol{S} :\ \Lambda_{\alpha,\beta} \to \frac{1}{2} \sum_{\alpha',\beta'=0,1/2} e^{4\pi i(\alpha\beta' + \beta\alpha')} \Lambda_{\alpha',\beta'}. \tag{10}$$

Note that, under $\boldsymbol{S}$ transformation, the combinations $\Lambda_{0,0} + \Lambda_{0,1/2}$ and $\Lambda_{1/2,0} - \Lambda_{1/2,1/2}$ are invariant and $\Lambda_{0,0} - \Lambda_{0,1/2}$ and $\Lambda_{1/2,0} + \Lambda_{1/2,1/2}$ are exchanged with each other.

Next, let us check the behaviors of $\Lambda_{\alpha,\beta}$ as $a \to 0$ ($R \to \infty$) and as $a \to \infty$ ($R \to 0$). For the $a \to 0$ limit, it is the part with zero coefficients of a^{-2} in the exponential in Eq. (8) that gives non-vanishing contributions. So only the lattices containing zero winding number are non-vanishing in the large-R limit:

$$(\eta\bar{\eta})^{-1} \sum_{n\in \boldsymbol{Z}} \exp\left[-\pi\, (a(n+\alpha))^2\right] \to (\eta\bar{\eta})^{-1} \int_{-\infty}^{\infty} \frac{dx}{a} e^{-\pi\tau_2 x^2} = \left(a\sqrt{\tau_2}\eta\bar{\eta}\right)^{-1}, \tag{11}$$

where $x = a(n+\alpha)$. Consequently, we see as $a \to 0$

$$\Lambda_{\alpha,0} \to \left(a\sqrt{\tau_2}\eta\bar{\eta}\right)^{-1},\ \ \Lambda_{\alpha,1/2} \to 0. \tag{12}$$

On the other hand, in the $a \to \infty$ limit, the non-vanishing contributions come from the lattices with zero momentum in Eq. (8):

$$(\eta\bar{\eta})^{-1} \sum_{w\in \boldsymbol{Z}} \exp\left[-4\pi \left(\frac{w+\beta}{a}\right)^2\right] \to (\eta\bar{\eta})^{-1} \int_{-\infty}^{\infty} \frac{dy}{a} e^{-4\pi\tau_2 y^2} = a\left(2\sqrt{\tau_2}\eta\bar{\eta}\right)^{-1}, \tag{13}$$

[2] It is not essential that a half translation $\mathcal{T}$ is accompanied with the T-dualized coordinate $\tilde{X}^9$. If we adopted the ordinary coordinate X^9, the sum in Eq. (8) would be over $n \in 2(\boldsymbol{Z} + \alpha)$ and $w \in \boldsymbol{Z} + \beta$.

where $y = (w+\beta)/a$. Consequently, we see as $a \to \infty$

$$\Lambda_{0,\beta} \to a\left(2\sqrt{\tau_2}\eta\bar{\eta}\right)^{-1}, \quad \Lambda_{1/2,\beta} \to 0. \tag{14}$$

Coming back to Eq. (6), we can rewrite it as

$$Z_+^{(9)+} = \left(\Lambda_{0,0} + \Lambda_{0,1/2}\right) Z_B^{(7)} Z_+^+, \tag{15}$$

using $\Lambda_{\alpha,\beta}$. An interpolating model is obtained from $Z_+^{(9)+}$ by orbifolding with the $\boldsymbol{Z}_2$ action $\mathcal{T}Q$. A half translation $\mathcal{T}$ affects the lattices $\Lambda_{\alpha,\beta}$ and acts such that only the states with even winding numbers survive:

$$\mathcal{T}Q: \; Z_+^{(9)+} \to Z_-^{(9)+} = \left(\Lambda_{0,0} - \Lambda_{0,1/2}\right) Z_B^{(7)} Z_-^+, \tag{16}$$

where Z_-^+ is defined as the Q action of Z_+^+. The modular invariance requires the twisted sector [27,28]. By using Eq. (10), we see that under $\boldsymbol{S}$ transformation, $Z_-^{(9)+}$ transforms as

$$\boldsymbol{S}: \; Z_-^{(9)+} \to Z_+^{(9)-} = \left(\Lambda_{1/2,0} + \Lambda_{1/2,1/2}\right) Z_B^{(7)} Z_+^-, \tag{17}$$

where $Z_-^+(-1/\tau) \equiv Z_+^-(\tau)$. Furthermore, when $\mathcal{T}Q$ acts on $Z_+^{(9)-}$, we obtain

$$\mathcal{T}Q: \; Z_-^{(9)+} \to Z_-^{(9)-} = \left(\Lambda_{1/2,0} - \Lambda_{1/2,1/2}\right) Z_B^{(7)} Z_-^-, \tag{18}$$

where Z_-^- is defined as the Q action of Z_+^-. As a result, the total partition function, which is modular invariant, is

$$\begin{aligned} Z_{\rm int}^{(9)} &= \frac{1}{2}\left(Z_+^{(9)+} + Z_-^{(9)+} + Z_+^{(9)-} + Z_-^{(9)-}\right) \\ &= \frac{1}{2} Z_B^{(7)} \left\{\Lambda_{0,0}\left(Z_+^+ + Z_-^+\right) + \Lambda_{0,1/2}\left(Z_+^+ - Z_-^+\right)\right. \\ &\qquad \left. + \Lambda_{1/2,0}\left(Z_+^- + Z_-^-\right) + \Lambda_{1/2,1/2}\left(Z_+^- - Z_-^-\right)\right\}. \end{aligned} \tag{19}$$

In accordance with Eq. (14), we see that $Z_{\rm int}^{(9)}$ reproduces model M_1 in the $a \to \infty$ limit. Note that the original model is reproduced as $R \to 0$ as we have adopted the convention that a half translation $\mathcal{T}$ is introduced with regard to the T-dualized coordinate. If $\mathcal{T}$ were introduced with regard to the ordinary coordinate, the interpolating model would reproduce the original model M_1 in the $R \to \infty$ limit. On the other hand, in the $a \to 0$ limit, $Z_{\rm int}^{(9)}$ produces model M_2 whose partition function is

$$Z_{M_2} = Z_B^{(8)}\left(Z_+^+ + Z_-^+ + Z_+^- + Z_-^-\right). \tag{20}$$

That is, model M_2 is obtained by Q-twisting model M_1, which means that model M_2 is related to model M_1 by the $\boldsymbol{Z}_2$ action Q.

2.2. *Two examples*

In this subsection, we review two examples of 9D interpolating models that are tachyon-free for all radii.

As the first example, let us choose the 10D $SO(16) \times SO(16)$ heterotic model as model M_1 and the 10D supersymmetric $SO(32)$ heterotic model as model M_2:

$$
\begin{aligned}
Z_{M_1} = Z_B^{(8)} \big\{ &\bar{O}_8 \left(V_{16}C_{16} + C_{16}V_{16}\right) + \bar{V}_8 \left(O_{16}O_{16} + S_{16}S_{16}\right) \\
&- \bar{S}_8 \left(V_{16}V_{16} + C_{16}C_{16}\right) - \bar{C}_8 \left(O_{16}S_{16} + S_{16}O_{16}\right) \big\},
\end{aligned} \tag{21}
$$

$$
Z_{M_2} = Z_B^{(8)} \left(\bar{V}_8 - \bar{S}_8\right) \left(O_{16}O_{16} + V_{16}V_{16} + S_{16}S_{16} + C_{16}C_{16}\right). \tag{22}
$$

In this case, in the language of Sect. 2.1,

$$
\begin{aligned}
Z_+^+ = {} & \bar{O}_8 \left(V_{16}C_{16} + C_{16}V_{16}\right) + \bar{V}_8 \left(O_{16}O_{16} + S_{16}S_{16}\right) \\
& - \bar{S}_8 \left(V_{16}V_{16} + C_{16}C_{16}\right) - \bar{C}_8 \left(O_{16}S_{16} + S_{16}O_{16}\right).
\end{aligned} \tag{23}
$$

The $\boldsymbol{Z}_2$ action Q that relates the $SO(16) \times SO(16)$ model to the supersymmetric $SO(32)$ model is $\bar{R}_{OC}$, which is defined as the reflection of the right-moving $SO(8)$ characters:

$$
\bar{R}_{OC} : \left(\bar{O}_8, \bar{V}_8, \bar{S}_8, \bar{C}_8\right) \to \left(-\bar{O}_8, \bar{V}_8, \bar{S}_8, -\bar{C}_8\right). \tag{24}
$$

Using this $\boldsymbol{Z}_2$ action Q and the modular transformation of $SO(2n)$ characters

$$
\boldsymbol{S} : \begin{pmatrix} O_{2n} \\ V_{2n} \\ S_{2n} \\ C_{2n} \end{pmatrix} \to \begin{pmatrix} 1 & 1 & 1 & 1 \\ 1 & 1 & -1 & -1 \\ 1 & -1 & i^n & -i^n \\ 1 & -1 & -i^n & i^n \end{pmatrix} \begin{pmatrix} O_{2n} \\ V_{2n} \\ S_{2n} \\ C_{2n} \end{pmatrix}, \tag{25}
$$

we have

$$
\begin{aligned}
Z_-^+ = {} & -\bar{O}_8 \left(V_{16}C_{16} + C_{16}V_{16}\right) + \bar{V}_8 \left(O_{16}O_{16} + S_{16}S_{16}\right) \\
& - \bar{S}_8 \left(V_{16}V_{16} + C_{16}C_{16}\right) + \bar{C}_8 \left(O_{16}S_{16} + S_{16}O_{16}\right), \\
Z_+^- = {} & \bar{O}_8 \left(O_{16}S_{16} + S_{16}O_{16}\right) + \bar{V}_8 \left(V_{16}V_{16} + C_{16}C_{16}\right) \\
& - \bar{S}_8 \left(O_{16}O_{16} + S_{16}S_{16}\right) - \bar{C}_8 \left(V_{16}C_{16} + C_{16}V_{16}\right), \\
Z_-^- = {} & -\bar{O}_8 \left(O_{16}S_{16} + S_{16}O_{16}\right) + \bar{V}_8 \left(V_{16}V_{16} + C_{16}C_{16}\right) \\
& - \bar{S}_8 \left(O_{16}O_{16} + S_{16}S_{16}\right) + \bar{C}_8 \left(V_{16}C_{16} + C_{16}V_{16}\right).
\end{aligned} \tag{26}
$$

Thus, from Eq. (19), we obtain the partition function of the interpolating model:

$$
\begin{aligned}
Z_{\mathrm{int}}^{(9)} = Z_B^{(7)} \big\{ &\Lambda_{0,0} \left(\bar{V}_8 \left(O_{16}O_{16} + S_{16}S_{16}\right) - \bar{S}_8 \left(V_{16}V_{16} + C_{16}C_{16}\right)\right) \\
&+ \Lambda_{0,1/2} \left(\bar{O}_8 \left(V_{16}C_{16} + C_{16}V_{16}\right) - \bar{C}_8 \left(O_{16}S_{16} + S_{16}O_{16}\right)\right) \\
&+ \Lambda_{1/2,0} \left(\bar{V}_8 \left(V_{16}V_{16} + C_{16}C_{16}\right) - \bar{S}_8 \left(O_{16}O_{16} + S_{16}S_{16}\right)\right) \\
&+ \Lambda_{1/2,1/2} \left(\bar{O}_8 \left(O_{16}S_{16} + S_{16}O_{16}\right) - \bar{C}_8 \left(V_{16}C_{16} + C_{16}V_{16}\right)\right) \big\}.
\end{aligned} \tag{27}
$$

We can see that the first and third lines of Eq. (27) reproduce the non-supersymmetric $SO(16) \times SO(16)$ model (21) while the first and second lines reproduce the supersymmetric $SO(32)$ model (22). Note that this interpolating model is tachyon-free for a generic radius because there are no such terms as $\bar{O}_8 O_{16} V_{16}$ or $\bar{O}_8 V_{16} O_{16}$ in the partition function (27).

Let us see the massless spectrum of this model from the partition function (27). For a generic radius $0 < R < \infty$, massless states can appear only when $n = w = 0$, so we can find the massless states by expanding the first line of Eq. (27) in q. We list the expansion of each character in Appendix B.1. Then, for a generic radius, the massless spectrum of the model is

- the 9D gravity multiplet: graviton $G_{\mu\nu}$, anti-symmetric tensor $B_{\mu\nu}$, and dilaton ϕ;
- the gauge bosons transforming in the adjoint representation of $SO(16) \times SO(16) \times U(1)^2_{G,B}$;
- a spinor transforming in the $(\mathbf{16}, \mathbf{16})$ of $SO(16) \times SO(16)$,

where $U(1)_{G,B}$ implies the Abelian factors generated by $G_{\mu 9}$ and $B_{\mu 9}$. Note that this model has no points at which the gauge symmetry is enhanced in the region $0 < R < \infty$. Also, there are no points at which the cosmological constant is exponentially suppressed, i.e., $N_F = N_B$, in all regions except $R \to \infty$. In the $R \to \infty$ limit, the number of fermions is equal to that of bosons at each mass level including the massless level, which means that SUSY is restored in the limit.

In the second example, let us choose the $SO(16) \times SO(16)$ heterotic model as model M_1 and the supersymmetric $E_8 \times E_8$ heterotic model as model M_2; Z_{M_1} is the same as in the first example and

$$Z_{M_2} = Z_B^{(8)} Z_+^+ = Z_B^{(8)} \left(\bar{V}_8 - \bar{S}_8\right) (O_{16} + S_{16}) (O_{16} + S_{16}). \tag{28}$$

In this case, the $\boldsymbol{Z}_2$ action Q is R_{VC}, which is defined as the reflection of one of the two left-moving $SO(16)$ characters:

$$R_{VC}: \ (O_{16}, V_{16}, S_{16}, C_{16}) \to (O_{16}, -V_{16}, S_{16}, -C_{16}). \tag{29}$$

The partition function of this interpolating model is obtained in a similar way to the first example:

$$\begin{aligned} Z^{(9)}_{\text{int}} = Z_B^{(7)} \big\{ & \Lambda_{0,0} \left(\bar{V}_8 \left(O_{16}O_{16} + S_{16}S_{16}\right) - \bar{S}_8 \left(O_{16}S_{16} + S_{16}O_{16}\right)\right) \\ & + \Lambda_{1/2,0} \left(\bar{V}_8 \left(O_{16}S_{16} + S_{16}O_{16}\right) - \bar{S}_8 \left(O_{16}O_{16} + S_{16}S_{16}\right)\right) \\ & + \Lambda_{0,1/2} \left(\bar{O}_8 \left(V_{16}C_{16} + C_{16}V_{16}\right) - \bar{C}_8 \left(V_{16}V_{16} + C_{16}C_{16}\right)\right) \\ & + \Lambda_{1/2,1/2} \left(\bar{O}_8 \left(V_{16}V_{16} + C_{16}C_{16}\right) - \bar{C}_8 \left(V_{16}C_{16} + C_{16}V_{16}\right)\right) \big\}. \end{aligned} \tag{30}$$

For a generic radius $0 < R < \infty$, the massless spectrum of this model is

- the 9D gravity multiplet: graviton $G_{\mu\nu}$, anti-symmetric tensor $B_{\mu\nu}$, and dilaton ϕ;
- the gauge bosons transforming in the adjoint representation of $SO(16) \times SO(16) \times U(1)^2_{G,B}$;
- a spinor transforming in the $(\mathbf{128}, \mathbf{1}) \oplus (\mathbf{1}, \mathbf{128})$ of $SO(16) \times SO(16)$.

In this case, there are no points either where the gauge symmetry is enhanced or the cosmological constant is exponentially suppressed.

3. Interpolating models with a Wilson line

The 9D interpolating models with the radius parameter R in Sect. 2 do not give us a model with $N_F = N_B$ no matter how we adjust R. We need to increase the number of parameters in order to search for such a model. We can realize $N_F - N_B = 0$ by compactifying more dimensions and adjusting the parameters of the compact manifold. For example, if the 9D model constructed in the previous example, in which $N_F - N_B = 64$, is compactified on a $(d-1)$-dimensional torus and the parameters of the torus are adjusted such that $U(1)^{2d}_{G,B}$ is enhanced to $U(1)^{2d-r}_{G,B} \times G$, where G is a rank-r group, which has eight non-zero roots, then we obtain interpolating models in which $N_F - N_B = 0$. However, in this work, we will add one parameter by turning on a Wilson line. In other words, we will generalize interpolating models by considering a twisted circle with a constant background. We expect that there are some conditions between parameters under which the gauge symmetry is enhanced as in Refs. [29–32]. In this section, we construct 9D interpolating models with two parameters by considering the compactification on a twisted circle with a Wilson line.

Let us write the uncompactified dimensions as X^μ ($\mu = 0, \ldots, 9$) and the internal ones as X_L^I ($I = 1, \ldots, 16$) for a 10D heterotic string model, and compactify the X^9-direction on a twisted circle. Furthermore, we switch on a constant Wilson line background with the components of $\mu = 9$ and $I = 1$ by adding to the worldsheet action

$$A \int d^2 z \bar{\partial} X^{\mu=9} \partial X_L^{I=1}. \tag{31}$$

It is only the momentum lattice of the center-of-mass mode that is affected by turning on the Wilson line A. The addition of the constant Wilson line background corresponds to a boost on the momentum lattice [29,30,33]:

$$\begin{pmatrix} \ell_L \\ p_L \\ p_R \end{pmatrix} \to \begin{pmatrix} \ell'_L \\ p'_L \\ p'_R \end{pmatrix} = R_{\ell_L\text{–}p_L} M_{\ell_L\text{–}p_R} \begin{pmatrix} \ell_L \\ p_L \\ p_R \end{pmatrix}, \tag{32}$$

where

$$\ell_L = \frac{1}{\sqrt{\alpha'}} m \tag{33}$$

is the left-moving momentum of the $X_L^{I=1}$-direction and $m \in \boldsymbol{Z}$ for the NS (Neveu–Schwarz, anti-periodic) boundary condition and $m \in \boldsymbol{Z} + 1/2$ for R (Ramond, periodic). Here, $M_{\ell_L\text{–}p_R}$ and $R_{\ell_L\text{–}p_L}$ represent the boost on the ℓ_L–p_R plane and the rotation on the ℓ_L–p_L plane respectively. The boost $M_{\ell_L\text{–}p_R}$ is written in terms of A as follows:

$$M_{\ell_L\text{–}p_R} = \begin{pmatrix} \sqrt{1+A^2} & 0 & A \\ 0 & 1 & 0 \\ A & 0 & \sqrt{1+A^2} \end{pmatrix}. \tag{34}$$

We use A to write $R_{\ell_L\text{–}p_L}$ as follows:

$$R_{\ell_L\text{–}p_L} = \begin{pmatrix} \frac{1}{\sqrt{1+A^2}} & -\frac{A}{\sqrt{1+A^2}} & 0 \\ \frac{A}{\sqrt{1+A^2}} & \frac{1}{\sqrt{1+A^2}} & 0 \\ 0 & 0 & 1 \end{pmatrix}. \tag{35}$$

Therefore, after turning on the Wilson line, we have

$$\begin{aligned} \ell'_L &= \frac{1}{\sqrt{2\alpha'}} \left(\sqrt{2} m - 2 \frac{A}{\sqrt{1+A^2}} \frac{w}{a} \right), \\ p'_L &= \frac{1}{\sqrt{2\alpha'}} \left(\sqrt{2} A m + \sqrt{1+A^2} a n + \frac{1-A^2}{\sqrt{1+A^2}} \frac{w}{a} \right), \\ p'_L &= \frac{1}{\sqrt{2\alpha'}} \left(\sqrt{2} A m + \sqrt{1+A^2} a n - \sqrt{1+A^2} \frac{w}{a} \right). \end{aligned} \tag{36}$$

The above equations mean that the left- and right-moving momenta of $X^{\mu=9}$ in Eq. (5) and the left-moving momentum of $X_L^{I=1}$ in Eq. (33) are mixed with each other by the Wilson line. In terms of the functions in the partition function, the momentum lattice and a theta function in one of the two left-moving $SO(16)$ characters are convoluted as follows:

$$\Lambda_{\alpha,\beta}\left(\frac{\vartheta\begin{bmatrix}\gamma\\ \delta\end{bmatrix}}{\eta}\right)^8 \to \Lambda^{(\alpha,\beta)}_{(\gamma,\delta)}(a,A)\left(\frac{\vartheta\begin{bmatrix}\gamma\\ \delta\end{bmatrix}}{\eta}\right)^7. \tag{37}$$

Here, we define $\Lambda^{(\alpha,\beta)}_{(\gamma,\delta)}$ by

$$\Lambda^{(\alpha,\beta)}_{(\gamma,\delta)}(a,A) \equiv (\eta\bar{\eta})^{-1}\,\eta^{-1}\sum_{n,w,m}(-1)^{2m\delta}q^{\frac{\alpha'}{2}(p_L'^2+\ell_L'^2)}\bar{q}^{\frac{\alpha'}{2}p_R'^2}, \tag{38}$$

where the sum is taken over $n\in \boldsymbol{Z}+\alpha$, $w\in 2(\boldsymbol{Z}+\beta)$, $m\in\boldsymbol{Z}+\gamma$. Substituting Eq. (36) into Eq. (38), we obtain

$$\Lambda^{(\alpha,\beta)}_{(\gamma,\delta)}(a,A) = (\eta\bar{\eta})^{-1}\,\eta^{-1}\sum_{\boldsymbol{n}\in\boldsymbol{Z}^3}\exp\left[-\pi\,(\boldsymbol{n}+\boldsymbol{x})^T M(\tau_1,\tau_2;a,A)\,(\boldsymbol{n}+\boldsymbol{x}) + 2\pi i\boldsymbol{y}\cdot\boldsymbol{n}\right], \tag{39}$$

where $\boldsymbol{n}^T=(n,w,m)$, $\boldsymbol{x}^T=(\alpha,\beta,\gamma)$, $\boldsymbol{y}^T=(0,0,\delta)$, and $M(\tau_1,\tau_2;a,A)$ is a 3×3 symmetric matrix of the following form:

$$M(\tau_1,\tau_2;a,A)=\begin{pmatrix} a^2\sqrt{1+A^2}\tau_2 & -2\left(A^2\tau_2+i\tau_1\right) & \sqrt{2}aA\sqrt{1+A^2}\tau_2 \\ -2\left(A^2\tau_2+i\tau_1\right) & 4a^{-2}\sqrt{1+A^2}\tau_2 & -2\sqrt{2}a^{-1}A\sqrt{1+A^2}\tau_2 \\ \sqrt{2}aA\sqrt{1+A^2}\tau_2 & -2\sqrt{2}a^{-1}A\sqrt{1+A^2}\tau_2 & (1+2A^2)\tau_2-i\tau_1 \end{pmatrix}. \tag{40}$$

It is easy to see that, under $\boldsymbol{T}:\ \tau\to\tau+1$,

$$\begin{aligned}\Lambda^{(\alpha,\beta)}_{(0,\delta)} &\to e^{4\pi i\alpha\beta}\Lambda^{(\alpha,\beta)}_{(0,\delta+1/2)},\\ \Lambda^{(\alpha,\beta)}_{(1/2,\delta)} &\to e^{4\pi i\alpha\beta}e^{\pi i/4}\Lambda^{(\alpha,\beta)}_{(1/2,\delta+1/2)}.\end{aligned} \tag{41}$$

Under $\boldsymbol{S}:\ \tau\to -1/\tau$, by using the Poisson resummation formula, we obtain

$$\Lambda^{(\alpha,\beta)}_{(\gamma,\delta)} \to \frac{1}{2}e^{2\pi i\gamma\delta}\sum_{\alpha',\beta'=0,1/2}e^{4\pi i(\alpha\beta'+\beta\alpha')}\Lambda^{(\alpha',\beta')}_{(\delta,\gamma)}. \tag{42}$$

Before introducing some examples, let us discuss the symmetry of the interpolating model. It is convenient to introduce a modular parameter $\tilde{\tau}$ in terms of the parameter of the twisted circle and Wilson line as

$$\tilde{\tau}=\tilde{\tau}_1+i\tilde{\tau}_2=\frac{A}{\sqrt{1+A^2}}\frac{1}{a}+i\frac{1}{\sqrt{1+A^2}}\frac{1}{a}. \tag{43}$$

Note that $|\tilde{\tau}|^2 = 1/a^2$, which means that the radial coordinate corresponds to radius R and the angular coordinate to Wilson line A. Using $\tilde{\tau}$, the momenta (36) are rewritten as

$$\begin{aligned}
\ell'_L &= \frac{1}{\sqrt{2\alpha'}}\left(\sqrt{2}m - 2\tilde{\tau}_1 w\right),\\
p'_L &= \frac{1}{\sqrt{2\alpha'}}\frac{1}{\tilde{\tau}_2}\left(\sqrt{2}\tilde{\tau}_1 m + n - (\tilde{\tau}_1^2 - \tilde{\tau}_2^2)w\right),\\
p'_L &= \frac{1}{\sqrt{2\alpha'}}\frac{1}{\tilde{\tau}_2}\left(\sqrt{2}\tilde{\tau}_1 m + n - (\tilde{\tau}_1^2 + \tilde{\tau}_2^2)w\right),
\end{aligned}\tag{44}$$

for $m \in \boldsymbol{Z} + \gamma$, $n \in \boldsymbol{Z} + \alpha$, $w \in 2(\boldsymbol{Z} + \beta)$. From these momenta (44), we can see that the lattice $\Lambda^{(\alpha,\beta)}_{(\gamma,\delta)}$ is invariant under the shift

$$\tilde{\tau} \to \tilde{\tau} + \sqrt{2} \tag{45}$$

with the redefinitions

$$m \to m' = m - 2w, \quad n \to n' = n + 2m - 2w, \quad w \to w' = w. \tag{46}$$

Therefore the fundamental region of moduli space is[3]

$$-\frac{\sqrt{2}}{2} \le \tilde{\tau}_1 \le \frac{\sqrt{2}}{2}. \tag{47}$$

3.1. *The interpolation between SUSY $SO(32)$ and $SO(16) \times SO(16)$*

As an example, let us include the Wilson line in the first example of Sect. 2.2. According to Eq. (37), the circle compactification of the $SO(16) \times SO(16)$ heterotic model with the Wilson line is

$$\begin{aligned}
Z^{(9)}_{SO(16)\times SO(16)}(a, A) &= Z^{(9)+}_{+}(a, A)\\
&= Z^{(7)}_B \sum_{\beta=0,1/2}\Big\{\bar{O}_8\left(V^{(0,\beta)}_{16}(a,A)C_{16} + C^{(0,\beta)}_{16}(a,A)V_{16}\right)\\
&\qquad + \bar{V}_8\left(O^{(0,\beta)}_{16}(a,A)O_{16} + S^{(0,\beta)}_{16}(a,A)S_{16}\right)\\
&\qquad - \bar{S}_8\left(V^{(0,\beta)}_{16}(a,A)V_{16} + C^{(0,\beta)}_{16}(a,A)C_{16}\right)\\
&\qquad - \bar{C}_8\left(O^{(0,\beta)}_{16}(a,A)S_{16} + S^{(0,\beta)}_{16}(a,A)O_{16}\right)\Big\},
\end{aligned}\tag{48}$$

where $O^{(\alpha,\beta)}_{2n}$, $V^{(\alpha,\beta)}_{2n}$, $S^{(\alpha,\beta)}_{2n}$, $C^{(\alpha,\beta)}_{2n}$ are defined by

$$\begin{aligned}
O^{(\alpha,\beta)}_{2n}(a, A) &\equiv \frac{1}{2\eta^{n-1}}\left(\Lambda^{(\alpha,\beta)}_{(0,0)}(a,A)\vartheta_3^{n-1} + \Lambda^{(\alpha,\beta)}_{(0,1/2)}(a,A)\vartheta_4^{n-1}\right),\\
V^{(\alpha,\beta)}_{2n}(a, A) &\equiv \frac{1}{2\eta^{n-1}}\left(\Lambda^{(\alpha,\beta)}_{(0,0)}(a,A)\vartheta_3^{n-1} - \Lambda^{(\alpha,\beta)}_{(0,1/2)}(a,A)\vartheta_4^{n-1}\right),
\end{aligned}$$

[3] If the $\boldsymbol{Z}_2$ twist $\mathcal{T}Q$ acted trivially, then n and w would both be integers. Then, in addition to the shift (45), the momentum lattices would be invariant under $\tilde{\tau} \to -1/\tilde{\tau}$ with the replacement $n \leftrightarrow w$. This transformation would correspond to a T-dual transformation, so the two limiting 10D models would be the same and the fundamental region would become $-\sqrt{2}/2 \le \tilde{\tau}_1 \le \sqrt{2}/2$ and $|\tilde{\tau}| \ge 1$.

$$S_{2n}^{(\alpha,\beta)}(a,A) \equiv \frac{1}{2\eta^{n-1}}\left(\Lambda_{(1/2,0)}^{(\alpha,\beta)}(a,A)\vartheta_2^{n-1} + \Lambda_{(1/2,1/2)}^{(\alpha,\beta)}(a,A)\vartheta_1^{n-1}\right),$$
$$C_{2n}^{(\alpha,\beta)}(a,A) \equiv \frac{1}{2\eta^{n-1}}\left(\Lambda_{(1/2,0)}^{(\alpha,\beta)}(a,A)\vartheta_2^{n-1} - \Lambda_{(1/2,1/2)}^{(\alpha,\beta)}(a,A)\vartheta_1^{n-1}\right). \tag{49}$$

We will refer to $O_n^{(\alpha,\beta)}$, $V_n^{(\alpha,\beta)}$, $S_n^{(\alpha,\beta)}$, $C_n^{(\alpha,\beta)}$ as boosted characters. In analogy with Sect. 2, the interpolating model can be constructed from Eq. (48) by orbifolding with the $\boldsymbol{Z}_2$ twist $\mathcal{T}Q$. In this case, $Q = \bar{R}_{OC}$ and the $\mathcal{T}$ action on the boosted characters changes the overall sign for $\beta = 1/2$. Using Eq. (42), we find that under an $\boldsymbol{S}$ transformation, the boosted characters transform as

$$\begin{pmatrix} O_{2n}^{(\alpha,\beta)} \\ V_{2n}^{(\alpha,\beta)} \\ S_{2n}^{(\alpha,\beta)} \\ C_{2n}^{(\alpha,\beta)} \end{pmatrix} \to \frac{1}{2}\sum_{\alpha',\beta'=0,1/2} e^{4\pi i(\alpha\beta'+\beta\alpha')} \begin{pmatrix} 1 & 1 & 1 & 1 \\ 1 & 1 & -1 & -1 \\ 1 & -1 & i^n & -i^n \\ 1 & -1 & -i^n & i^n \end{pmatrix} \begin{pmatrix} O_{2n}^{(\alpha',\beta')} \\ V_{2n}^{(\alpha',\beta')} \\ S_{2n}^{(\alpha',\beta')} \\ C_{2n}^{(\alpha',\beta')} \end{pmatrix}. \tag{50}$$

We obtain

$$\begin{aligned}
Z_-^{(9)+} &= Z_B^{(7)} \sum_{\beta=0,1/2} e^{2\pi i\beta}\Big\{-\bar{O}_8\left(V_{16}^{(0,\beta)}C_{16} + C_{16}^{(0,\beta)}V_{16}\right) + \bar{V}_8\left(O_{16}^{(0,\beta)}O_{16} + S_{16}^{(0,\beta)}S_{16}\right) \\
&\qquad -\bar{S}_8\left(V_{16}^{(0,\beta)}V_{16} + C_{16}^{(0,\beta)}C_{16}\right) + \bar{C}_8\left(O_{16}^{(0,\beta)}S_{16} + S_{16}^{(0,\beta)}O_{16}\right)\Big\}, \\
Z_+^{(9)-} &= Z_B^{(7)} \sum_{\beta=0,1/2} \Big\{\bar{O}_8\left(O_{16}^{(1/2,\beta)}S_{16} + S_{16}^{(1/2,\beta)}O_{16}\right) + \bar{V}_8\left(V_{16}^{(1/2,\beta)}V_{16} + C_{16}^{(1/2,\beta)}C_{16}\right) \\
&\qquad -\bar{S}_8\left(O_{16}^{(1/2,\beta)}O_{16} + S_{16}^{(1/2,\beta)}S_{16}\right) - \bar{C}_8\left(V_{16}^{(1/2,\beta)}C_{16} + C_{16}^{(1/2,\beta)}V_{16}\right)\Big\}, \\
Z_-^{(9)-} &= Z_B^{(7)} \sum_{\beta=0,1/2} e^{2\pi i\beta}\Big\{-\bar{O}_8\left(O_{16}^{(1/2,\beta)}S_{16} + S_{16}^{(1/2,\beta)}O_{16}\right) + \bar{V}_8\left(V_{16}^{(1/2,\beta)}V_{16} + C_{16}^{(1/2,\beta)}C_{16}\right) \\
&\qquad -\bar{S}_8\left(O_{16}^{(1/2,\beta)}O_{16} + S_{16}^{(1/2,\beta)}S_{16}\right) + \bar{C}_8\left(V_{16}^{(1/2,\beta)}C_{16} + C_{16}^{(1/2,\beta)}V_{16}\right)\Big\}.
\end{aligned} \tag{51}$$

As a result of these equations, we find the total partition function of the interpolating model:

$$\begin{aligned}
Z_{\text{int}}^{(9)}(a,A) &= \frac{1}{2}Z_B^{(7)}\left(Z_+^{(9)+} + Z_-^{(9)+} + Z_+^{(9)-} + Z_-^{(9)-}\right) \\
&= Z_B^{(7)}\Big\{\bar{V}_8\left(O_{16}^{(0,0)}O_{16} + S_{16}^{(0,0)}S_{16}\right) - \bar{S}_8\left(V_{16}^{(0,0)}V_{16} + C_{16}^{(0,0)}C_{16}\right) \\
&\quad + \bar{O}_8\left(V_{16}^{(0,1/2)}C_{16} + C_{16}^{(0,1/2)}V_{16}\right) - \bar{C}_8\left(O_{16}^{(0,1/2)}S_{16} + S_{16}^{(0,1/2)}O_{16}\right) \\
&\quad + \bar{V}_8\left(V_{16}^{(1/2,0)}V_{16} + C_{16}^{(1/2,0)}C_{16}\right) - \bar{S}_8\left(O_{16}^{(1/2,0)}O_{16} + S_{16}^{(1/2,0)}S_{16}\right) \\
&\quad + \bar{O}_8\left(O_{16}^{(1/2,1/2)}S_{16} + S_{16}^{(1/2,1/2)}O_{16}\right) - \bar{C}_8\left(V_{16}^{(1/2,1/2)}C_{16} + C_{16}^{(1/2,1/2)}V_{16}\right)\Big\}.
\end{aligned} \tag{52}$$

Note that the only difference between Eq. (27) and Eq. (52) is that the momentum lattices are mixed with one of the two left-moving $SO(16)$ characters. Of course, it is easy to check that Eq. (52) is equal to Eq. (27) when $A = 0$.

3.1.1. The limiting cases

Next, let us see the limiting cases $a \to 0$ and $a \to \infty$ of the interpolating model (52). In the partition function (52), only the momentum lattices (38) depend on a, so we need to see the behavior of $\Lambda^{(\alpha,\beta)}_{(\gamma,\delta)}$ in these limiting cases. As in the cases without a Wilson line, the non-vanishing contributions come from the parts with zero winding number (momentum) in the $a \to 0$ ($a \to \infty$) limit, and $\Lambda^{(\alpha,1/2)}_{(\gamma,\delta)}$ ($\Lambda^{(1/2,\beta)}_{(\gamma,\delta)}$) vanishes as $a \to 0$ ($a \to \infty$). As $a \to 0$, we find

$$\begin{aligned}
\Lambda^{(\alpha,0)}_{(\gamma,\delta)}(a,A) &\underset{w=0}{\simeq} (\eta\bar{\eta})^{-1}\eta^{-1}\sum_{n,m\in\boldsymbol{Z}} q^{(m+\gamma)^2/2}e^{2\pi i m\delta} \\
&\qquad \times \exp\left[-\pi\tau_2(1+A^2)\left(a(n+\alpha)+\sqrt{2}\frac{A}{\sqrt{1+A^2}}(m+\gamma)\right)^2\right] \\
&\to (\eta\bar{\eta})^{-1}\eta^{-1}\sum_{m\in\boldsymbol{Z}} q^{(m+\gamma)^2/2}e^{2\pi i m\delta}\int_{-\infty}^{\infty}\frac{dx}{a}e^{-\pi\tau_2(1+A^2)x^2} \\
&= \frac{R_\infty}{\sqrt{\alpha'\tau_2}}(\eta\bar{\eta})^{-1}\eta^{-1}\vartheta\begin{bmatrix}\gamma\\ \delta\end{bmatrix},
\end{aligned} \tag{53}$$

where $x \equiv a(n+\alpha)+\sqrt{2}A(m+\gamma)/\sqrt{1+A^2}$ and $R_\infty \equiv R/\sqrt{1+A^2}$. Similarly as $a \to \infty$, we find

$$\begin{aligned}
\Lambda^{(0,\beta)}_{(\gamma,\delta)}(a,A) &\underset{n=0}{\simeq} (\eta\bar{\eta})^{-1}\eta^{-1}\sum_{w,m\in\boldsymbol{Z}} q^{(m+\gamma)^2/2}e^{2\pi i m\delta} \\
&\qquad \times \exp\left[-4\pi\tau_2(1+A^2)\left(\frac{w+\alpha}{a}-\frac{1}{\sqrt{2}}\frac{A}{\sqrt{1+A^2}}(m+\gamma)\right)^2\right] \\
&\to (\eta\bar{\eta})^{-1}\eta^{-1}\sum_{m\in\boldsymbol{Z}} q^{(m+\gamma)^2/2}e^{2\pi i m\delta}a\int_{-\infty}^{\infty}dy e^{-4\pi\tau_2(1+A^2)y^2} \\
&= \frac{\sqrt{\alpha'}}{2\sqrt{\tau_2}R_0}(\eta\bar{\eta})^{-1}\eta^{-1}\vartheta\begin{bmatrix}\gamma\\ \delta\end{bmatrix},
\end{aligned} \tag{54}$$

where $y \equiv (w+\alpha)/a - A(m+\gamma)/\sqrt{2(1+A^2)}$ and $R_0 \equiv \sqrt{1+A^2}R$. Note that R_∞ (R_0) is the physical radius at the large- (small-) R region. In fact, from Eq. (36) we see

$$\begin{aligned}
\left(\ell'^2_L + p'^2_L\right)\big|_{m=w=0} &= p'^2_R\big|_{m=w=0} = \frac{1}{2}\left(\frac{n}{R_\infty}\right)^2, \\
\left(\ell'^2_L + p'^2_L\right)\big|_{m=n=0} &= p'^2_R\big|_{m=n=0} = \frac{1}{2}\left(\frac{wR_0}{\alpha'}\right)^2.
\end{aligned} \tag{55}$$

Note that the effect of the Wilson line is found only with the physical radii in the limiting cases. In terms of the boosted characters, Eq. (53) and Eq. (54) respectively imply

$$\begin{aligned}
(O_n,V_n,S_n,C_n)^{(\alpha,\beta)} &\to \frac{R_\infty}{\sqrt{\alpha'\tau_2}}(\eta\bar{\eta})^{-1}\eta^{-1}\left(O_n,V_n,S_n,C_n\right)\delta_{\beta,0} \qquad (a\to 0), \\
(O_n,V_n,S_n,C_n)^{(\alpha,\beta)} &\to \frac{\sqrt{\alpha'}}{2\sqrt{\tau_2}R_0}(\eta\bar{\eta})^{-1}\eta^{-1}\left(O_n,V_n,S_n,C_n\right)\delta_{\alpha,0} \qquad (a\to \infty).
\end{aligned} \tag{56}$$

Thus, Eq. (56) shows that the interpolating model (52) provides the $SO(16) \times SO(16)$ model at $a \to 0$ and the supersymmetric $SO(32)$ model at $a \to \infty$ for any value of the Wilson line A.

3.1.2. The massless spectrum

Let us see the massless spectrum of this interpolating model for a generic set of values of a and A. As is done in Sect. 2, we can identify massless states from the parts with zero momentum and zero winding number of the partition function (52). By expanding the characters in q,[4] we find the following massless states for a generic set of values of a and A:

- the 9D gravity multiplet: graviton $G_{\mu\nu}$, anti-symmetric tensor $B_{\mu\nu}$, and dilaton ϕ;
- the gauge bosons transforming in the adjoint representation of $SO(16) \times SO(14) \times U(1) \times U(1)^2_{G,B}$;
- a spinor transforming in the $(\mathbf{16}, \mathbf{14})$ of $SO(16) \times SO(14)$.

Note that, compared to the first example in Sect. 2.2, the gauge symmetry is broken to $SO(16) \times SO(14) \times U(1)$ because of the Wilson line, and $N_F - N_B = 32$.

There are some conditions under which the additional massless states appear:

(I) $\tilde{\tau}_1 = n_1/\sqrt{2} \quad (n_1 \in \boldsymbol{Z})$

Using a and A, this condition is rewritten as

$$\sqrt{2}A + \sqrt{1 + A^2}an_1 = 0, \tag{57}$$

for any integer n_1. Under this condition, we find that the following additional massless states appear:

- two vectors transforming in the $(\mathbf{1}, \mathbf{14})$ of $SO(16) \times SO(14)$;
- two spinors transforming in the $(\mathbf{16}, \mathbf{1})$ of $SO(16) \times SO(14)$.

These massless vectors and spinors come from $\bar{V}_8 O^{(0,0)}_{16} O_{16}$ and $\bar{S}_8 V^{(0,0)}_{16} V_{16}$ respectively when $(m, n) = (\pm 1, \pm n_1)$ and $w = 0$. This condition 4 thus enhances the gauge symmetry to $SO(16) \times SO(16) \times U(1)^2_{G,B}$, and at the same time, the massless spinor is promoted to transform in the $(\mathbf{16}, \mathbf{16})$ of $SO(16) \times SO(16)$ as well. In this case, the additional massless fermionic and bosonic degrees of freedom are 256 and 224 respectively, and $N_F - N_B = 64$.

Note that condition 4 does not mean an infinite number of gauge-enhanced orbits on the $\tilde{\tau}$ plane. Recalling the fundamental region (47) of the interpolating model, condition 4 implies that there are only two inequivalent $SO(16) \times SO(16)$ orbits. One of them is the $n_1 = 0$ orbit, which corresponds to the case $A = 0$. Thus, this orbit reproduces the first example in Sect. 2.2. The other is the $n_1 = 1$ ($n_1 = -1$) orbit, which is the new one that does not appear before considering the constant Wilson line background.

(II) $\tilde{\tau}_1 = n_2/\sqrt{2} \quad (n_2 \in \boldsymbol{Z} + 1/2)$

Under this condition, we find that the following additional massless states appear:

- two vectors transforming in the $(\mathbf{16}, \mathbf{1})$ of $SO(16) \times SO(14)$;
- two spinors transforming in the $(\mathbf{1}, \mathbf{14})$ of $SO(16) \times SO(14)$.

These massless vectors and spinors come from $\bar{V}_8 V^{(1/2,0)}_{16} V_{16}$ and $\bar{S}_8 O^{(1/2,0)}_{16} O_{16}$ respectively when $(m, n) = (\pm 1, \pm n_2)$ and $w = 0$. This condition 4 thus enhances the gauge symmetry to

[4] We list the expansion of the boosted characters (49) in q in Appendix B.2.

Table 1. We summarize the conditions under which the additional massless states appear. The cosmological constant is exponentially suppressed when the gauge group is enhanced to $SO(14) \times SO(18)$.

Conditions	$\tilde{\tau}_1 = n_1/\sqrt{2}$ $(n_1 \in \boldsymbol{Z})$	$\tilde{\tau}_1 = n_2/\sqrt{2}$ $(n_2 \in \boldsymbol{Z} + 1/2)$
Gauge group	$SO(16) \times SO(16)$	$SO(14) \times SO(18)$
$N_F - N_B$	positive	zero

$SO(18) \times SO(14) \times U(1)^2_{G,B}$, and at the same time, the massless spinor is promoted to transform in the $(\mathbf{18}, \mathbf{14})$ of $SO(18) \times SO(14)$ as well. In this case, the additional massless fermionic and bosonic degrees of freedom are 224 and 256 respectively, which means that $N_F - N_B = 0$. The cosmological constant is exponentially suppressed on these orbits.

Note that there are only two inequivalent orbits on which condition 4 is satisfied. For any half-integer n_2, all orbits are related either to the one with $n_2 = 1/2$ or the one with $n_2 = -1/2$ by the shift (45).

(III) $\frac{1}{\sqrt{2}}\tilde{\tau}_1 - \left(\tilde{\tau}_1^2 + \tilde{\tau}_2^2\right) w_3 = 0 \quad (w_2 \in 2\boldsymbol{Z} + 1)$

Using a and A, this condition is rewritten as

$$\frac{1}{\sqrt{2}}A - \sqrt{1 + A^2}\frac{w_3}{a} = 0, \tag{58}$$

for any odd integer w_3. The additional massless states are

- two conjugate spinors transforming in the $(\mathbf{1}, \mathbf{64})$ of $SO(16) \times SO(14)$.

These massless conjugate spinors come from $\bar{C}_8 S_{16}^{(0,0)} O_{16}$ when $(m, w) = (\pm 1/2, \pm w_3)$ and $n = 0$. Note that these conjugate spinors are the remnants of the $\mathbf{8}_C \otimes (\mathbf{1}, \mathbf{128})$ in the 10D $SO(16) \times SO(16)$ model.

We plot these conditions in the fundamental region (47) of $\tilde{\tau}$ plane in Fig. 1. Table 1 summarizes the conditions under which the additional massless states appear in this model. The table shows only the conditions with $w = 0$ because we are interested in the large-R region where Eq. (1) is valid.

3.2. *The interpolation between $E_8 \times E_8$ and $SO(16) \times SO(16)$*

Next, let us include the Wilson line in the second example of Sect. 2.2. The starting point is the same as in Sect. 3.1 but the Q action is R_{VC} in this case. According to the construction in Sect. 2.1, we find that the total partition function is

$$\begin{aligned} Z_{\mathrm{int}}^{(9)}(a, A) &= \frac{1}{2} Z_B^{(7)} \left(Z_+^{(9)+} + Z_-^{(9)+} + Z_+^{(9)-} + Z_-^{(9)-}\right) \\ &= Z_B^{(7)} \Big\{ \bar{V}_8 \left(O_{16}^{(0,0)} O_{16} + S_{16}^{(0,0)} S_{16}\right) - \bar{S}_8 \left(O_{16}^{(0,0)} S_{16} + S_{16}^{(0,0)} O_{16}\right) \\ &\quad + \bar{O}_8 \left(V_{16}^{(0,1/2)} C_{16} + C_{16}^{(0,1/2)} V_{16}\right) - \bar{C}_8 \left(V_{16}^{(0,1/2)} V_{16} + C_{16}^{(0,1/2)} C_{16}\right) \\ &\quad + \bar{V}_8 \left(O_{16}^{(1/2,0)} S_{16} + S_{16}^{(1/2,0)} O_{16}\right) - \bar{S}_8 \left(O_{16}^{(1/2,0)} O_{16} + S_{16}^{(1/2,0)} S_{16}\right) \\ &\quad + \bar{O}_8 \left(V_{16}^{(1/2,1/2)} V_{16} + C_{16}^{(1/2,1/2)} C_{16}\right) - \bar{C}_8 \left(V_{16}^{(1/2,1/2)} C_{16} + C_{16}^{(1/2,1/2)} V_{16}\right) \Big\}. \end{aligned} \tag{59}$$

Using the limiting behaviors of the boosted characters (56), we can see that this interpolating model (59) reproduces the supersymmetric $E_8 \times E_8$ model and the $SO(16) \times SO(16)$ model as $a \to 0$ and $a \to \infty$ respectively, for any value of A.

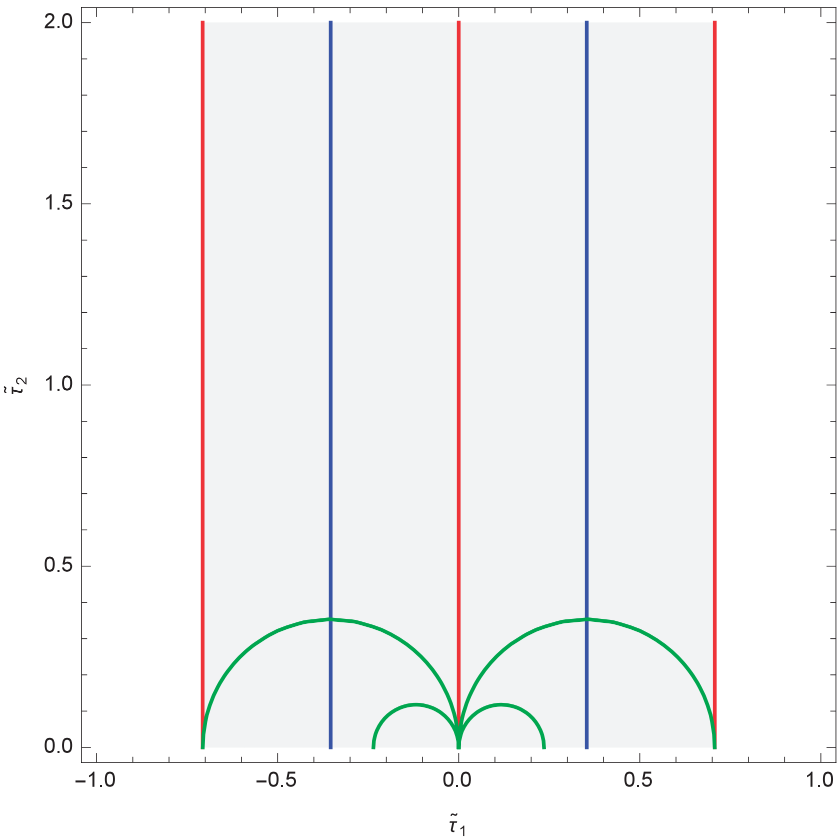

Fig. 1. The shaded region is the fundamental region (47) and we plot the orbits on which the additional massless states appear in the first example. The three red lines correspond to condition 4 under which the gauge symmetry is enhanced to $SO(16) \times SO(16)$, and the one in the center implies the case of $A = 0$. The two blue lines correspond to condition 4 under which the gauge symmetry is enhanced to $SO(18) \times SO(14)$. The green semicircles correspond to condition 4 and we plot four orbits with $w_3 = \pm 1, \pm 3$.

3.2.1. The massless spectrum

Let us see the massless spectrum of this interpolating model for a generic set of values of a and A. By expanding the partition function (59) in q, we find

- the 9D gravity multiplet: graviton $G_{\mu\nu}$, anti-symmetric tensor $B_{\mu\nu}$, and dilaton ϕ;
- the gauge bosons transforming in the adjoint representation of $SO(16) \times SO(14) \times U(1) \times U(1)^2_{G,B}$;
- a spinor transforming in the $(\mathbf{128}, \mathbf{1})$ of $SO(16) \times SO(14)$.

These massless states come from $\bar{V}_8 O^{(0,0)}_{16} O_{16}$ or $\bar{S}_8 O^{(0,0)}_{16} S_{16}$. For a generic set of values of a and A, $N_F - N_B = -736$, and the cosmological constant becomes negative. We find that there are some conditions between a and A under which the additional massless states appear:

(I) $\tilde{\tau}_1 = n_1/\sqrt{2} \quad (n_1 \in \boldsymbol{Z})$

Under this condition, we find that the following additional massless states appear:

- two vectors transforming in the $(\mathbf{1}, \mathbf{14})$ of $SO(16) \times SO(14)$.

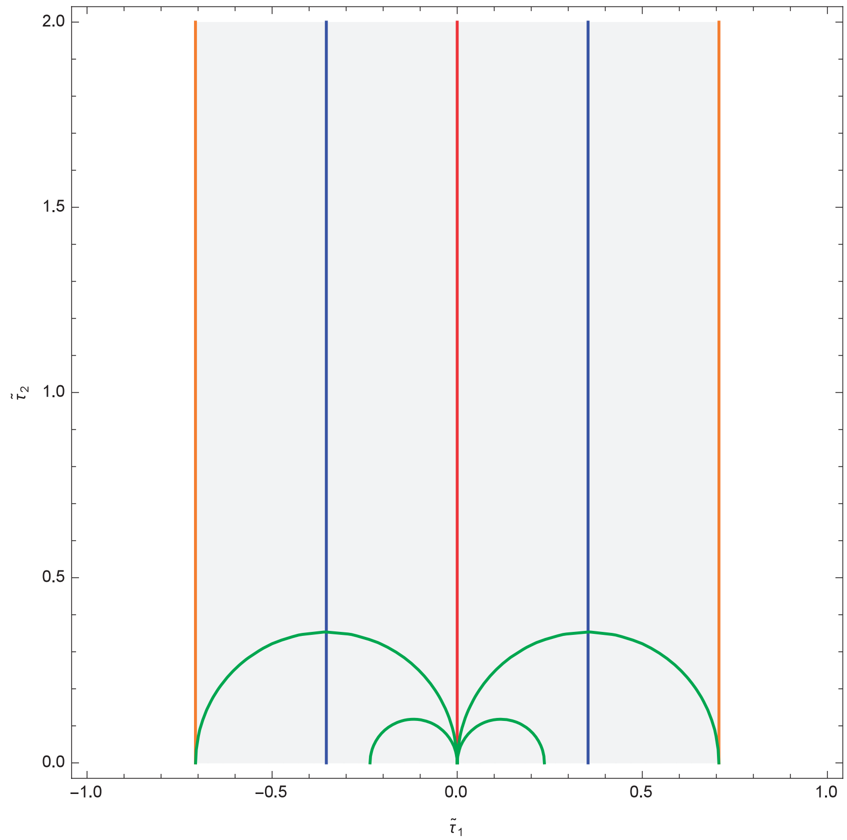

Fig. 2. The shaded region is the fundamental region (47) and we plot the orbits on which additional massless states appear in the second example. The red line corresponds to condition (I) under which the gauge symmetry is enhanced to $SO(16) \times SO(16)$. The two orange lines correspond to condition (I) under which the gauge symmetry is enhanced to $SO(16) \times E_8$. The two blue lines correspond to condition (I). The green semicircles correspond to condition (I) and we plot four orbits with $w_3 = \pm 1, \pm 3$.

These massless vectors come from $\bar{V}_8 O_{16}^{(0,0)} O_{16}$ when $(m, n) = (\pm 1, \pm n_1)$ and $w = 0$. This condition (I) thus enhances the gauge symmetry to $SO(16) \times SO(16) \times U(1)^2_{G,B}$. Furthermore, different additional massless states appear depending on whether n_1 is even or odd:

(I-a) $n_1 \in 2\boldsymbol{Z}$

- two spinors transforming in the $(\mathbf{1}, \mathbf{64})$ of $SO(16) \times SO(14)$.

These states come from $\bar{S}_8 S_{16}^{(0,0)} O_{16}$ when $(m, n) = (\pm 1/2, \pm n_1/2)$ and $w = 0$. In the representation of the $SO(16) \times SO(16)$, this is a spinor transforming in the $(\mathbf{1}, \mathbf{128})$. Note that in the fundamental region (47), this condition corresponds to the $\tilde{\tau}_1 = 0$ orbit, which means the case $A = 0$. The massless spectrum under this condition is thus the same as that of the second example in Sect. 2.2.

(I-b) $n_1 \in 2\boldsymbol{Z} + 1$

- two vectors transforming in the $(\mathbf{1}, \mathbf{64})$ of $SO(16) \times SO(14)$.

These states come from $\bar{V}_8 S_{16}^{(1/2,0)} O_{16}$ when $(m, n) = (\pm 1/2, \pm n_1/2)$ and $w = 0$. In representation of the $SO(16) \times SO(16)$, this is a vector transforming in the $(\mathbf{1}, \mathbf{128})$. Therefore, under this condition, the gauge symmetry is enhanced to $SO(16) \times E_8$ beyond $SO(16) \times SO(16)$. Note that in the fundamental region (47), this condition corresponds to the $\tilde{\tau}_1 = \sqrt{2}/2$ (or $\tilde{\tau}_1 = -\sqrt{2}/2$) orbit.

Table 2. We summarize the condition under which the additional massless states appear. In this model, there is no condition where the cosmological constant is exponentially suppressed.

Conditions	$\tilde{\tau}_1 = n_1/\sqrt{2}$ $(n_1 \in 2\boldsymbol{Z})$	$\tilde{\tau}_1 = n_1/\sqrt{2}$ $(n_1 \in 2\boldsymbol{Z}+1)$	$\tilde{\tau}_1 = n_2/\sqrt{2}$ $(n_2 \in \boldsymbol{Z}+1/2)$
Gauge group	$SO(16) \times SO(16)$	$SO(16) \times E_8$	$SO(16) \times SO(14) \times U(1)$
$N_F - N_B$	positive	negative	negative

(II) $\tilde{\tau}_1 = n_2/\sqrt{2} \quad (n_2 \in \boldsymbol{Z} + 1/2)$

Under this condition, we find that the following additional massless states appear:

- two spinors transforming in the $(\mathbf{1}, \mathbf{14})$ of $SO(16) \times SO(14)$.

These massless spinors come from $\bar{S}_8 O_{16}^{(1/2,0)} O_{16}$ when $(m, n) = (\pm 1, \pm n_2)$ and $w = 0$. Note that in the fundamental region (47), this condition corresponds to the two orbits, which are $\tilde{\tau}_1 = \sqrt{2}/4$ and $\tilde{\tau}_1 = -\sqrt{2}/4$.

(III) $\frac{1}{\sqrt{2}}\tilde{\tau}_1 - \left(\tilde{\tau}_1^2 + \tilde{\tau}_2^2\right) w_3 = 0 \quad (w_3 \in 2\boldsymbol{Z} + 1)$

The additional massless states are

- two conjugate spinors transforming in the $(\mathbf{16}, \mathbf{1})$ of $SO(16) \times SO(14)$.

These massless conjugate spinors come from $\bar{C}_8 V_{16}^{(0,1/2)} V_{16}$ when $(m, w) = (\pm 1/2, \pm w_3)$ and $n = 0$. Note that these conjugate spinors are the remnants of the $\mathbf{8}_C \otimes (\mathbf{16}, \mathbf{16})$ in the 10D $SO(16) \times SO(16)$ model.

We plot these conditions in the fundamental region (47) of the $\tilde{\tau}$ plane in Fig. 2. Table 2 summarizes the conditions under which the additional massless states appear in this model.

Finally, let us mention that in these models considered in this section, it is straightforward to calculate tree and one-loop scattering amplitudes of massless particles to obtain signals of broken supersymmetry [34–37].

4. Conclusions

We have constructed 9D interpolating models with two parameters by considering the compactification on a twisted circle with a constant Wilson line background (31), and have studied the massless spectra of these models. Furthermore, we have found some conditions between circle radius R and Wilson line A under which additional massless states are present. In the 9D model that interpolates between the 10D supersymmetric $SO(32)$ model and the 10D $SO(16) \times SO(16)$ model, we find the conditions under which the gauge symmetry is enhanced to $SO(16) \times SO(16)$ or $SO(18) \times SO(14)$. In particular, under the second condition, the massless fermionic and bosonic degrees of freedom become equal, which means that the cosmological constant is exponentially suppressed. Recent references related to this point include Refs. [38–40]. According to Ref. [41], which is carried out in the type I dual picture [42], the brane configuration with the gauge group $SO(18) \times SO(14)$ yields a 9D non-supersymmetric model with $N_F - N_B = 0$, although it has tachyonic directions in moduli space. On the other hand, our interpolation between the 10D supersymmetric $E_8 \times E_8$ model and the 10D $SO(16) \times SO(16)$ model did not produce a condition with $N_F - N_B = 0$. We have, however, found the conditions under which the gauge symmetry is enhanced to $SO(16) \times SO(16)$ or $SO(16) \times E_8$.

As part of our future work, we have to discuss the stability of the Wilson line as in Refs. [38–41]. Even if the cosmological constant is very small on a certain point (orbit) of moduli space, it is not clear that the Wilson line is stable on the point (orbit). Namely, we need to write down the cosmological constant in terms of the Wilson line and find the stable points of the Wilson line.

Acknowledgements

The work of H.I. was partially supported by Japan Society for the Promotion of Science (JSPS) KAKENHI Grant Number 19K03828.

Funding

Open Access funding: SCOAP^3.

Appendix A. Notation for the partition functions

We summarize the notation for some functions that appear in the partition functions. The Dedekind eta function is

$$\eta(\tau) = q^{-1/24} \prod_{n=1}^{\infty} \left(1 - q^n\right), \tag{A.60}$$

where $q = e^{2\pi i \tau}$. The theta function with characteristics is defined by

$$\vartheta \begin{bmatrix} \alpha \\ \beta \end{bmatrix} (z, \tau) = \sum_{n=-\infty}^{\infty} \exp\left(\pi i (n+\alpha)^2 \tau + 2\pi i (n+\alpha)(z+\beta)\right). \tag{A.61}$$

In particular, when α and β are 0 or 1/2 and $z = 0$, we use the following shorthand notations:

$$\vartheta_1(\tau) = \vartheta \begin{bmatrix} 1/2 \\ 1/2 \end{bmatrix} (0, \tau) = 0, \tag{A.62}$$

$$\vartheta_2(\tau) = \vartheta \begin{bmatrix} 1/2 \\ 0 \end{bmatrix} (0, \tau), \tag{A.63}$$

$$\vartheta_3(\tau) = \vartheta \begin{bmatrix} 0 \\ 0 \end{bmatrix} (0, \tau), \tag{A.64}$$

$$\vartheta_4(\tau) = \vartheta \begin{bmatrix} 0 \\ 1/2 \end{bmatrix} (0, \tau). \tag{A.65}$$

These theta functions satisfy the Jacobi's abstruse identity:

$$\vartheta_3(\tau)^4 - \vartheta_4(\tau)^4 - \vartheta_2(\tau)^4 = 0. \tag{A.66}$$

We write the $SO(2n)$ characters in terms of the theta functions as follows:

$$O_{2n} = \frac{1}{2\eta^n} \left(\vartheta_3^n + \vartheta_4^n\right), \tag{A.67}$$

$$V_{2n} = \frac{1}{2\eta^n} \left(\vartheta_3^n - \vartheta_4^n\right), \tag{A.68}$$

$$S_{2n} = \frac{1}{2\eta^n} \left(\vartheta_2^n + \vartheta_1^n\right), \tag{A.69}$$

$$C_{2n} = \frac{1}{2\eta^n} \left(\vartheta_2^n - \vartheta_1^n\right). \tag{A.70}$$

In terms of the characters, the Jacobi's abstruse identity is

$$V_8 - S_8 = 0. \tag{A.71}$$

Appendix B. The expansions of the characters

In string theories, we can see the spectrum of each mass level by expanding the partition function in q. In this appendix, in order to see the massless states, which are the coefficients of q^0, we shall expand the $SO(8)$ and $SO(16)$ characters, which appear in the partition function of some heterotic models[5].

Appendix B.1. The case with no Wilson line

For Sect. 2, we expand $\eta^{-8}\,(O_{2n}, V_{2n}, S_{2n}, C_{2n})$ where η^8 is the contribution from X^m and the $SO(2n)$ characters are from ψ^m or X_L^I, where $m = 2, \ldots, 10$ and $I = 1, \ldots, 16$:

$$\eta^{-8} O_{2n} = q^{-8/24 - n/24} \left(1 + \frac{2n(2n-1)}{2} q + 8q + \mathcal{O}(q^2)\right), \tag{B.72}$$

$$\eta^{-8} V_{2n} = q^{-8/24 - n/24 + 1/2} \left(2n + \mathcal{O}(q)\right), \tag{B.73}$$

$$\eta^{-8} S_{2n} = \eta^{-8} C_{2n} = q^{-8/24 + n/12} \left(2^{n-1} + \mathcal{O}(q)\right). \tag{B.74}$$

Note that the lowest-order terms of Eqs. (B.72), (B.73), and (B.74) correspond to the degrees of freedom of the identity, the vector, and the spinor (the conjugate spinor) respectively, and the second term of Eq. (B.72) to the adjoint representation of $SO(2n)$. The third term of $\eta^{-8}O_{2n}$ comes from η^{-8}, i.e., the contributions from X^m.

The right-moving parts of the partition functions are expanded as

$$\bar{\eta}^{-8} \bar{O}_8 = \bar{q}^{-1/2} \left(1 + \frac{2n(2n-1)}{2} \bar{q} + 8\bar{q} + \mathcal{O}(\bar{q}^2)\right), \tag{B.75}$$

$$\bar{\eta}^{-8} \bar{V}_8 = 8 + \mathcal{O}(\bar{q}), \tag{B.76}$$

$$\bar{\eta}^{-8} \bar{S}_8 = \bar{\eta}^{-8} \bar{S}_8 = 8 + \mathcal{O}(\bar{q}). \tag{B.77}$$

The left-moving parts of the partition functions in some heterotic models might include

$$\eta^{-8} O_{16} O_{16} = q^{-1} \left(1 + 2 \cdot \frac{16 \cdot 15}{2} + 8q + \mathcal{O}(q^2)\right), \tag{B.78}$$

$$\eta^{-8} O_{16} V_{16} = q^{-1/2} \left(2n + \mathcal{O}(q)\right), \tag{B.79}$$

$$\eta^{-8} O_{16} S_{16} = \eta^{-8} O_{16} C_{16} = 2^{n-1} + \mathcal{O}(q), \tag{B.80}$$

$$\eta^{-8} V_{16} V_{16} = 16 \cdot 16 + \mathcal{O}(q), \tag{B.81}$$

$$\eta^{-8} V_{16} S_{16} = \eta^{-8} V_{16} C_{16} = q^{-1/2} \left(2n \cdot 2^{n-1} + \mathcal{O}(q)\right), \tag{B.82}$$

$$\eta^{-8} S_{16} S_{16} = \eta^{-8} S_{16} C_{16} = q \left(2^{2(n-1)} + \mathcal{O}(q)\right). \tag{B.83}$$

Note that all states that come from $\eta^{-8}V_{16}S_{16}$ or $\eta^{-8}S_{16}S_{16}$ ($\eta^{-8}S_{16}C_{16}$) are massive, and tachyons can appear only from the combination $(\eta\bar{\eta})^{-8}\,\bar{O}_8 O_{16} V_{16}$ because of the level-matching condition.

---

[5] There are five 10D heterotic models whose partition functions are expressed in terms of the characters $SO(8)$ or $SO(16)$: the supersymmetric $SO(32)$ model, the supersymmetric $E_8 \times E_8$ model, the non-supersymmetric $SO(32)$ model, the $SO(16) \times E_8$ model, the $SO(16) \times SO(16)$ model.

Appendix B.2. The case with the Wilson line

As in Sect. 3, when the Wilson line is switched on, the left-moving $SO(16)$ characters and the momentum lattices are mixed. So, in such a case, we need to expand the boosted characters (49) in order to see the spectrum. The boosted characters are expanded as follows:

$$
\begin{aligned}
O_{16}^{(\alpha,\beta)} &= \frac{1}{2\eta^7}\left(\Lambda^{(\alpha,\beta)}_{(0,0)}\vartheta_3^7 + \Lambda^{(\alpha,\beta)}_{(0,1/2)}\vartheta_4^7\right)\\
&= (\eta\bar{\eta})^{-1} q^{-\frac{8}{24}} \sum_{n,w}\left\{\sum_{m\in 2\boldsymbol{Z}} q^{\frac{\alpha'}{2}(\ell_L'^2+p_L'^2)}\bar{q}^{\frac{\alpha'}{2}p_R'^2}\left(1+q+\frac{14\cdot 13}{2}q+\mathcal{O}(q^{\frac{3}{2}})\right)\right.\\
&\qquad\left.+\sum_{m\in 2\boldsymbol{Z}+1} q^{\frac{\alpha'}{2}(\ell_L'^2+p_L'^2)}\bar{q}^{\frac{\alpha'}{2}p_R'^2}\left(14q^{\frac{1}{2}}+\mathcal{O}(q^{\frac{3}{2}})\right)\right\},\\
V_{16}^{(\alpha,\beta)} &= \frac{1}{2\eta^7}\left(\Lambda^{(\alpha,\beta)}_{(0,0)}\vartheta_3^7 - \Lambda^{(\alpha,\beta)}_{(0,1/2)}\vartheta_4^7\right)\\
&= (\eta\bar{\eta})^{-1} q^{-\frac{8}{24}} \sum_{n,w}\left\{\sum_{m\in 2\boldsymbol{Z}} q^{\frac{\alpha'}{2}(\ell_L'^2+p_L'^2)}\bar{q}^{\frac{\alpha'}{2}p_R'^2}\left(14q^{\frac{1}{2}}+\mathcal{O}(q^{\frac{3}{2}})\right)\right.\\
&\qquad\left.+\sum_{m\in 2\boldsymbol{Z}+1} q^{\frac{\alpha'}{2}(\ell_L'^2+p_L'^2)}\bar{q}^{\frac{\alpha'}{2}p_R'^2}\left(1+q+\frac{14\cdot 13}{2}q+\mathcal{O}(q^{\frac{3}{2}})\right)\right\},\\
S_{16}^{(\alpha,\beta)} = C_{16}^{(\alpha,\beta)} &= \frac{1}{2\eta^7}\left(\Lambda^{(\alpha,\beta)}_{(1/2,0)}\vartheta_2^7 \pm \Lambda^{(\alpha,\beta)}_{(1/2,1/2)}\vartheta_1^7\right)\\
&= (\eta\bar{\eta})^{-1} q^{-\frac{1}{24}+\frac{7}{12}} \sum_{n,w}\left\{\sum_{m\in \boldsymbol{Z}+1/2} q^{\frac{\alpha'}{2}(\ell_L'^2+p_L'^2)}\bar{q}^{\frac{\alpha'}{2}p_R'^2}\left(2^{7-1}+\mathcal{O}(q)\right)\right\},
\end{aligned}
\tag{B.84}
$$

where the sum is taken over $n \in \boldsymbol{Z}+\alpha$ and $w \in 2(\boldsymbol{Z}+\beta)$. As we are interested only in the left-moving parts of the partition function, we expand the following products:

$$
\begin{aligned}
&\bar{\eta}\eta^{-7} O_{16}^{(\alpha,\beta)} O_{16} = q^{-1}\sum_{n,w}\left\{\sum_{m\in 2\boldsymbol{Z}} q^{\frac{\alpha'}{2}(\ell_L'^2+p_L'^2)}\bar{q}^{\frac{\alpha'}{2}p_R'^2}\left(1+8q+\left(\frac{16\cdot 15}{2}+\frac{14\cdot 13}{2}+1\right)q+\mathcal{O}(q^{\frac{3}{2}})\right)\right.\\
&\qquad\left.+\sum_{m\in 2\boldsymbol{Z}+1} q^{\frac{\alpha'}{2}(\ell_L'^2+p_L'^2)}\bar{q}^{\frac{\alpha'}{2}p_R'^2}\left(1\cdot 14q^{\frac{1}{2}}+\mathcal{O}(q^{\frac{3}{2}})\right)\right\},\\
&\bar{\eta}\eta^{-7} O_{16}^{(\alpha,\beta)} V_{16}\\
&= q^{-\frac{1}{2}}\sum_{n,w}\left\{\sum_{m\in 2\boldsymbol{Z}} q^{\frac{\alpha'}{2}(\ell_L'^2+p_L'^2)}\bar{q}^{\frac{\alpha'}{2}p_R'^2}\left(16\cdot 1+\mathcal{O}(q)\right)+\sum_{m\in 2\boldsymbol{Z}+1} q^{\frac{\alpha'}{2}(\ell_L'^2+p_L'^2)}\bar{q}^{\frac{\alpha'}{2}p_R'^2}\left(16\cdot 14q^{\frac{1}{2}}+\mathcal{O}(q)\right)\right\},\\
&\bar{\eta}\eta^{-7} O_{16}^{(\alpha,\beta)} S_{16} = \bar{\eta}\eta^{-7} O_{16}^{(\alpha,\beta)} C_{16}\\
&= \sum_{n,w}\left\{\sum_{m\in 2\boldsymbol{Z}} q^{\frac{\alpha'}{2}(\ell_L'^2+p_L'^2)}\bar{q}^{\frac{\alpha'}{2}p_R'^2}\left(2^{8-1}\cdot 1+\mathcal{O}(q)\right)+\sum_{m\in 2\boldsymbol{Z}+1} q^{\frac{\alpha'}{2}(\ell_L'^2+p_L'^2)}\bar{q}^{\frac{\alpha'}{2}p_R'^2}\left(\mathcal{O}(q^{\frac{1}{2}})\right)\right\},
\end{aligned}
$$

$$\bar{\eta}\eta^{-7}V_{16}^{(\alpha,\beta)}O_{16} = q^{-1}\sum_{n,w}\left\{\sum_{m\in 2\boldsymbol{Z}} q^{\frac{\alpha'}{2}(\ell_L'^2+p_L'^2)}\bar{q}^{\frac{\alpha'}{2}p_R'^2}\left(1\cdot 14q^{\frac{1}{2}}+\mathcal{O}(q^{\frac{3}{2}})\right)\right.$$
$$\left.+\sum_{m\in 2\boldsymbol{Z}+1} q^{\frac{\alpha'}{2}(\ell_L'^2+p_L'^2)}\bar{q}^{\frac{\alpha'}{2}p_R'^2}\left(1+8q+\left(\frac{16\cdot 15}{2}+\frac{14\cdot 13}{2}+1\right)q+\mathcal{O}(q^{\frac{3}{2}})\right)\right\},$$

$$\bar{\eta}\eta^{-7}V_{16}^{(\alpha,\beta)}V_{16}$$
$$= q^{-\frac{1}{2}}\sum_{n,w}\left\{\sum_{m\in 2\boldsymbol{Z}} q^{\frac{\alpha'}{2}(\ell_L'^2+p_L'^2)}\bar{q}^{\frac{\alpha'}{2}p_R'^2}\left(16\cdot 14q^{\frac{1}{2}}+\mathcal{O}(q)\right)+\sum_{m\in 2\boldsymbol{Z}+1} q^{\frac{\alpha'}{2}(\ell_L'^2+p_L'^2)}\bar{q}^{\frac{\alpha'}{2}p_R'^2}\left(16\cdot 1+\mathcal{O}(q)\right)\right\},$$

$$\bar{\eta}\eta^{-7}V_{16}^{(\alpha,\beta)}S_{16} = \bar{\eta}\eta^{-7}V_{16}^{(\alpha,\beta)}C_{16}$$
$$= \sum_{n,w}\left\{\sum_{m\in 2\boldsymbol{Z}} q^{\frac{\alpha'}{2}(\ell_L'^2+p_L'^2)}\bar{q}^{\frac{\alpha'}{2}p_R'^2}\left(\mathcal{O}(q^{\frac{1}{2}})\right)+\sum_{m\in 2\boldsymbol{Z}+1} q^{\frac{\alpha'}{2}(\ell_L'^2+p_L'^2)}\bar{q}^{\frac{\alpha'}{2}p_R'^2}\left(2^{8-1}\cdot 1+\mathcal{O}(q)\right)\right\},$$

$$\bar{\eta}\eta^{-7}S_{16}^{(\alpha,\beta)}O_{16} = \bar{\eta}\eta^{-7}C_{16}^{(\alpha,\beta)}O_{16} = q^{-\frac{1}{8}}\sum_{n,w}\sum_{m\in\boldsymbol{Z}+1/2} q^{\frac{\alpha'}{2}(\ell_L'^2+p_L'^2)}\bar{q}^{\frac{\alpha'}{2}p_R'^2}\left(1\cdot 2^{7-1}+\mathcal{O}(q)\right),$$

$$\bar{\eta}\eta^{-7}S_{16}^{(\alpha,\beta)}V_{16} = \bar{\eta}\eta^{-7}C_{16}^{(\alpha,\beta)}V_{16} = q^{\frac{3}{8}}\sum_{n,w}\sum_{m\in\boldsymbol{Z}+1/2} q^{\frac{\alpha'}{2}(\ell_L'^2+p_L'^2)}\bar{q}^{\frac{\alpha'}{2}p_R'^2}\left(\mathcal{O}(1)\right),$$

$$\bar{\eta}\eta^{-7}S_{16}^{(\alpha,\beta)}S_{16} = \bar{\eta}\eta^{-7}C_{16}^{(\alpha,\beta)}S_{16} = \bar{\eta}\eta^{-7}S_{16}^{(\alpha,\beta)}C_{16} = \bar{\eta}\eta^{-7}C_{16}^{(\alpha,\beta)}C_{16}$$
$$= q^{\frac{7}{8}}\sum_{n,w}\sum_{m\in\boldsymbol{Z}+1/2} q^{\frac{\alpha'}{2}(\ell_L'^2+p_L'^2)}\bar{q}^{\frac{\alpha'}{2}p_R'^2}\left(\mathcal{O}(1)\right). \tag{B.85}$$

Note that no states that come from $S_{16}^{(\alpha,\beta)}S_{16}$ $(= S_{16}^{(\alpha,\beta)}C_{16} = C_{16}^{(\alpha,\beta)}S_{16} = C_{16}^{(\alpha,\beta)}C_{16})$ or $S_{16}^{(\alpha,\beta)}V_{16}$ $(= C_{16}^{(\alpha,\beta)}V_{16})$ will ever be massless.

References

[1] L. J. Dixon and J. A. Harvey, Nucl. Phys. B **274**, 93 (1986).
[2] L. Alvarez-Gaumé, P. Ginsparg, G. Moore, and C. Vafa, Phys. Lett. B **171**, 155 (1986).
[3] A. Font and A. Hernández, Nucl. Phys. B **634**, 51 (2002) [arXiv:hep-th/0202057] [Search INSPIRE].
[4] G. Moore, Nucl. Phys. B **293**, 139 (1987); **299**, 847 (1988) [erratum].
[5] J. Balog and M. P. Tuite, Nucl. Phys. B **319**, 387 (1989).
[6] K. R. Dienes, Phys. Rev. D **42**, 2004 (1990).
[7] T. R. Taylor, Nucl. Phys. B **303**, 543 (1988).
[8] Y. Satoh, Y. Sugawara, and T. Wada, J. High Energy Phys. **1602**, 184 (2016) [arXiv:1512.05155 [hep-th]] [Search INSPIRE].
[9] Y. Sugawara and T. Wada, J. High Energy Phys. **1608**, 028 (2016) [arXiv:1605.07021 [hep-th]] [Search INSPIRE].
[10] S. Kachru, J. Kumar, and E. Silverstein, Phys. Rev. D **59**, 106004 (1999) [arXiv:hep-th/9807076] [Search INSPIRE].
[11] S. Kachru and E. Silverstein, J. High Energy Phys. **9901**, 004 (1999) [arXiv:hep-th/9810129] [Search INSPIRE].
[12] H. Itoyama and T. R. Taylor, Phys. Lett. B **186**, 129 (1987).
[13] J. D. Blum and K. R. Dienes, Nucl. Phys. B **516**, 83 (1998) [arXiv:hep-th/9707160] [Search INSPIRE].
[14] S. Abel, K. R. Dienes, and E. Mavroudi, Phys. Rev. D **91**, 126014 (2015) [arXiv:1502.03087 [hep-th]] [Search INSPIRE].
[15] B. Aaronson, S. Abel, and E. Mavroudi, Phys. Rev. D **95**, 106001 (2017) [arXiv:1612.05742 [hep-th]] [Search INSPIRE].
[16] J. Scherk and J. H. Schwarz, Phys. Lett. B **82**, 60 (1979).

[17] R. Rohm, Nucl. Phys. B **237**, 553 (1984).
[18] K. Kikkawa and M. Yamasaki, Phys. Lett. B **149**, 357 (1984).
[19] N. Sakai and I. Senda, Prog. Theor. Phys. **75**, 692 (1986); **77**, 773 (1987) [erratum].
[20] H. Itoyama and T. R. Taylor, FERMILAB-CONF-87-129-T.
[21] S. Groot Nibbelink, O. Loukas, A. Mütter, E. Parr, and P. K. S. Vaudrevange, arXiv:1710.09237 [hep-th] [Search INSPIRE].
[22] S. Abel and R. J. Stewart, Phys. Rev. D **96**, 106013 (2017) [arXiv:1701.06629 [hep-th]] [Search INSPIRE].
[23] D. J. Gross, J. A. Harvey, E. Martinec, and R. Rohm, Phys. Rev. Lett. **54**, 502 (1985).
[24] H. Kawai, D. C. Lewellen, and S.-H. Henry Tye, Nucl. Phys. B **288**, 1 (1987).
[25] I. Antoniadis, C. P. Bachas, and C. Kounnas, Nucl. Phys. B **289**, 87 (1987).
[26] H. Kawai, D. C. Lewellen, and S.-H. H. Tye, Phys. Rev. D **34**, 3794 (1986).
[27] L. Dixon, J. A. Harvey, C. Vafa, and E. Witten, Nucl. Phys. B **261**, 678 (1985).
[28] L. Dixon, J. A. Harvey, C. Vafa, and E. Witten, Nucl. Phys. B **274**, 285 (1986).
[29] K. S. Narain, Phys. Lett. B **169**, 41 (1986).
[30] K. S. Narain, M. H. Sarmadi, and E. Witten, Nucl. Phys. B **279**, 369 (1987).
[31] P. Ginsparg and C. Vafa, Nucl. Phys. B **289**, 414 (1987).
[32] B. Fraiman, M. Graña, and C. A. Nuñez, J. High Energy Phys. **1809**, 078 (2018) [arXiv:1805.11128 [hep-th]] [Search INSPIRE].
[33] Y. Hamada, H. Kawai, and K.-y. Oda, Phys. Rev. D **92**, 045009 (2015) [arXiv:1501.04455 [hep-ph]] [Search INSPIRE].
[34] H. Itoyama and P. Moxhay, Nucl. Phys. B **293**, 685 (1987).
[35] H. Itoyama and K. Yano, Prog. Theor. Exp. Phys. **2016**, 033B05 (2016) [arXiv:1512.07705 [hep-th]] [Search INSPIRE].
[36] Y. Arakane, H. Itoyama, H. Kunitomo, and A. Tokura, Nucl. Phys. B **486**, 149 (1997) [arXiv:hep-th/9609151] [Search INSPIRE].
[37] V. A. Kostelecký, O. Lechtenfeld, W. Lerche, S. Samuel, and S. Watamura, Nucl. Phys. B **288**, 173 (1987).
[38] C. Kounnas and H. Partouche, Nucl. Phys. B **913**, 593 (2016) [arXiv:1607.01767 [hep-th]] [Search INSPIRE].
[39] C. Kounnas and H. Partouche, Nucl. Phys. B **919**, 41 (2017) [arXiv:1701.00545 [hep-th]] [Search INSPIRE].
[40] I. Florakis and J. Rizos, Nucl. Phys. B **913**, 495 (2016) [arXiv:1608.04582 [hep-th]] [Search INSPIRE].
[41] S. Abel, E. Dudas, D. Lewis, and H. Partouche, J. High Energy Phys. **1910**, 226 (2019) [arXiv:1812.09714 [hep-th]] [Search INSPIRE].
[42] J. Polchinski and E. Witten, Nucl. Phys. B **460**, 525 (1996) [arXiv:hep-th/9510169] [Search INSPIRE].